Supporting Information

Effects of the conjugated bridges on photovoltaic properties of *ortho*-functionalized perylene diimides for non-fullerene polymer solar cells

Jiazun Wu,‡[ab] Xiangchun Li,‡[c] Xiaodong Liu,*[ab] Shuanghong Wu,*[a] Wen-Yong Lai*[c] and Yonghao Zheng*[ab]

[a] *School of Optoelectronic Science and Engineering, University of Electronic Science and Technology of China (UESTC), Chengdu 610054, PR China. E-mail: xdliu@uestc.edu.cn; shwu@uestc.edu.cn; zhengyonghao@uestc.edu.cn*

[b] *Center for Applied Chemistry, University of Electronic Science and Technology of China (UESTC), Chengdu, 611731, PR China.*

[c] *Key Laboratory for Organic Electronics and Information Displays (KLOEID) & Institute of Advanced Materials (IAM), Jiangsu National Synergetic Innovation Center for Advanced Materials (SICAM), Nanjing University of Posts & Telecommunications, 9 Wenyuan Road, Nanjing 210023, PR China. E-mail: iamwylai@njupt.edu.cn*

‡ These authors contributed equally to this work.

Contents

1. Synthetic procedures

PDI-ThBr: Under nitrogen, magnesium turnings (72.0 mg, 3.0 mmol) were placed in a 50 mL round bottom flask. Anhydrous THF (10 mL) was added, followed by the addition of a catalytical amount of iodine. The 2-bromothiophene (450.0 mg, 2.8 mmol) was added dropwise to the reaction mixture that was heated to reflux until the brown color of iodine disappeared. The mixture was stirred for 3 hours and cooled to room temperature. Once the Grignard reagent had formed, 5 mL of thienylmagnesium bromide solution (1.4 mmol) was added to compound **PDI** (400.0 mg, 0.57 mmol) in THF (40 mL) at 0 °C. The resulting mixture was stirred at room temperature for 12 h and then quenched with water (5 mL). The product was extracted into DCM, the organic layers collected and dried with $MgSO_4$. The crude product was passed to a silica plug to remove the baseline. A mixture of crude product and N-bromosuccinimide (462.5 mg, 2.6 mmol) in 100 mL of dichloromethane was stirred at room temperature for 12 h. The crude product was purified by column chromatography on silica gel (DCM/Hexane, 1:1 v/v) to afford **PDI-ThBr** (200.8 mg, 41%). Mp: >260 °C. ^{1}H NMR(600 MHz, $CDCl_3$, δ, ppm): 8.58 (d, J = 7.9 Hz, 2H), 8.51 (d, J = 8.0 Hz, 2H), 8.44 (dd, J = 22.3, 8.0 Hz, 2H), 8.36 (s, 1H), 7.14 (d, J = 3.7 Hz, 1H), 7.01 (d, J = 3.7 Hz, 1H), 5.19-5.04 (m, 2H), 2.23 (dd, J = 9.4, 4.2 Hz, 4H), 1.92-1.77 (m, 4H), 1.57-1.03 (m, 24H), 0.83 (q, J = 6.7 Hz, 12H). ^{13}C NMR (151 MHz, $CDCl_3$, δ, ppm): 164.34, 163.36, 144.06, 138.60, 138.07, 134.04, 133.97, 133.20, 132.95, 132.06, 131.81, 131.72, 131.06, 130.30, 130.11, 129.33, 128.03, 127.92, 127.26, 126.14, 126.00, 125.53, 124.14, 123.93, 122.98, 122.91, 121.14, 114.08, 54.79, 54.77, 32.31, 32.14, 31.75, 31.63, 26.64, 26.60, 22.58, 22.56, 14.07, 14.05. Calcd for MS: 858.31,

Found: (M^+). 858.28. Anal. Calcd for $C_{50}H_{55}BrN_2O_4S$: C, 69.83; H, 6.45; N, 3.26. Found: C, 69.41; H, 6.01; N, 4.01.

PDI-2Th-PDI: Under nitrogen, **PDI-ThBr** (100.0 mg, 0.12 mmol), $NiCl_2$ (2.01 mg, 0.01 mmol), Zn (270.0 mg, 9.00 mmol) and PPh_3 (31.4 mg, 0.12 mmol) were dissolved in DMF (15 mL) and the solution was refluxed 24 h. The product was extracted into DCM, the organic layers collected and dried with $MgSO_4$. The crude product was purified by column chromatography on silica gel (DCM/Hexane, 1:1 v/v) to afford **PDI-2Th-PDI** (200.8 mg, 55%). Mp: >260 °C. ^{1}H NMR(600 MHz, $CDCl_3$, δ, ppm): 8.70 (s, 2H), 8.51 (dd, J = 27.2, 8.7 Hz, 10H), 8.40 (d, J = 7.8 Hz, 2H), 7.33 (d, J = 3.5 Hz, 2H), 7.23 (d, J = 3.0 Hz, 2H), 5.15 (d, J = 65.2 Hz, 4H), 2.24 (d, J = 37.3 Hz, 8H), 1.87 (s, 8H), 1.30 (tt, J = 24.8, 12.4 Hz, 48H), 0.86 (dt, J = 14.1, 6.9 Hz, 24H). ^{13}C NMR (151 MHz, $CDCl_3$, δ, ppm): 164.49, 164.21, 163.52, 163.23, 141.81, 139.21, 134.26, 133.81, 133.57, 133.05, 131.86, 131.55, 131.11, 130.78, 130.40, 129.41, 128.16, 128.01, 126.23, 126.16, 125.82, 124.40, 124.17, 123.97, 123.46, 123.23, 122.86, 121.18, 54.99, 54.82, 32.35, 32.19, 31.78, 29.61, 26.72, 26.67, 22.65, 22.57, 14.10, 14.04. Calcd for MS: 1558.78, Found: (M^+). 1558.67. Anal. Calcd for $C_{100}H_{110}N_4O_8S_2$: C, 76.99; H, 7.11; N, 3.59. Found: C, 77.42; H, 6.79; N, 4.02.

PDI-ThFTh-PDI: Under nitrogen, **PDI-ThBr** (180.0 mg, 0.21 mmol), **9,9-dioctylfluorene-2-bis(boronic acid pinacol ester)** (46.8 mg, 0.07 mmol), TBAB (20.4 mg, 0.06 mmol) and $Pd(PPh_3)_4$ (40.0 mg, 0.03 mmol) were dissolved in Toluene (12 mL) and the solution was refluxed. Then aqueous 2 M K_2CO_3 (4.0 mL) was added dropwise, and the mixture was stirred at 95 °C for 48 h. The product was extracted into DCM, the organic layers collected and dried with $MgSO_4$. The crude product was purified by column chromatography on silica gel (DCM/Hexane, 1:1 v/v) to afford **PDI-ThFTh-PDI** (245.3 mg, 60%). Mp: >260 °C. ^{1}H NMR(600 MHz, $CDCl_3$, δ, ppm):

8.75-8.58 (m, 14H), 7.74 (d, J = 7.9 Hz, 2H), 7.70 (d, J = 7.9 Hz, 2H), 7.67 (s, 2H), 7.51 (d, J = 3.6 Hz, 2H), 7.31 (s, 2H), 5.17 (d, J = 32.9 Hz, 4H), 2.24 (s, 8H), 2.08 (s, 4H), 1.85 (s, 8H), 1.24 (ddd, J = 96.5, 35.7, 12.3 Hz, 72H), 0.90-0.79 (m, 30H). ^{13}C NMR (151 MHz, $CDCl_3$, δ, ppm): 164.60, 163.92, 163.52, 163.12, 151.76, 147.15, 141.49, 140.57, 140.21, 134.47, 134.22, 134.00, 133.21, 133.07, 131.81, 131.16, 131.04, 130.66, 129.50, 128.52, 128.30, 126.41, 126.03, 124.97, 124.14, 123.93, 123.33, 123.18, 123.06, 122.97, 122.88, 120.24, 120.12, 119.99, 55.39, 54.78, 54.76, 40.65, 32.33, 32.21, 31.79, 31.77, 31.74, 30.12, 29.68, 29.37, 29.32, 29.27, 26.64, 26.62, 23.89, 22.62, 22.55, 14.08, 14.03. Calcd for MS: 1947.09, Found: (M^+). 1946.96. Anal. Calcd for $C_{129}H_{150}N_4O_8S_2$: C, 79.51; H, 7.76; N, 2.88. Found: C, 79.21; H, 8.05; N, 2.31.

2. Thermogravimetric analysis (TGA)

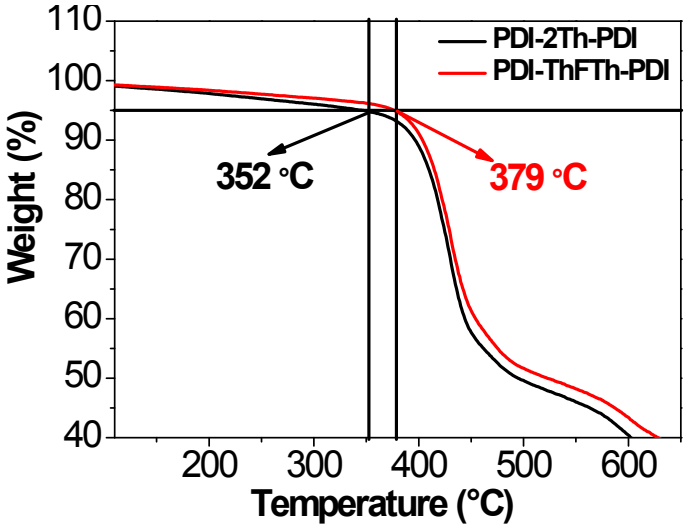

Fig. S1 TGA plots of PDI-2Th-PDI and PDI-ThFTh-PDI.

3. Photoluminescence (PL) spectra

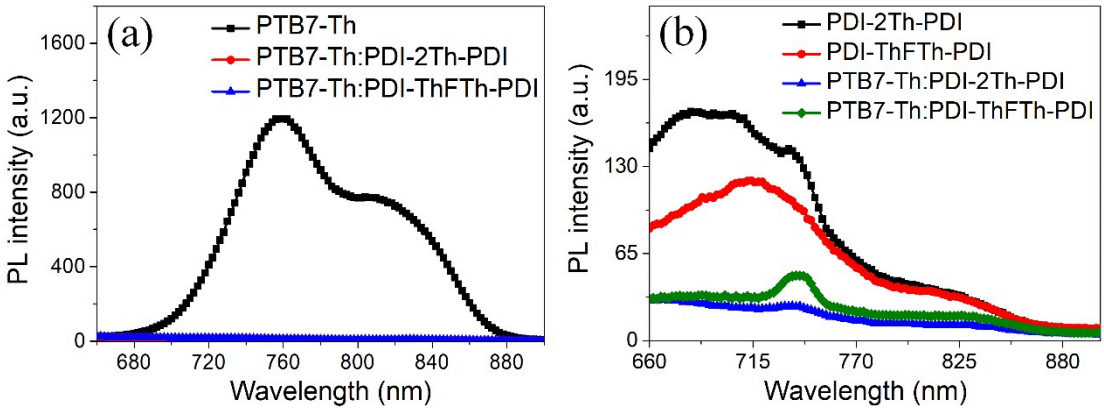

Fig. S2 Photoluminescence spectra of (a) PTB7-Th and PTB7-Th:acceptor blend films (excitation at 620 nm), and (b) two PDI acceptors and PTB7-Th:acceptor blend films (excitation at 490 nm).

4. Cyclic voltammograms

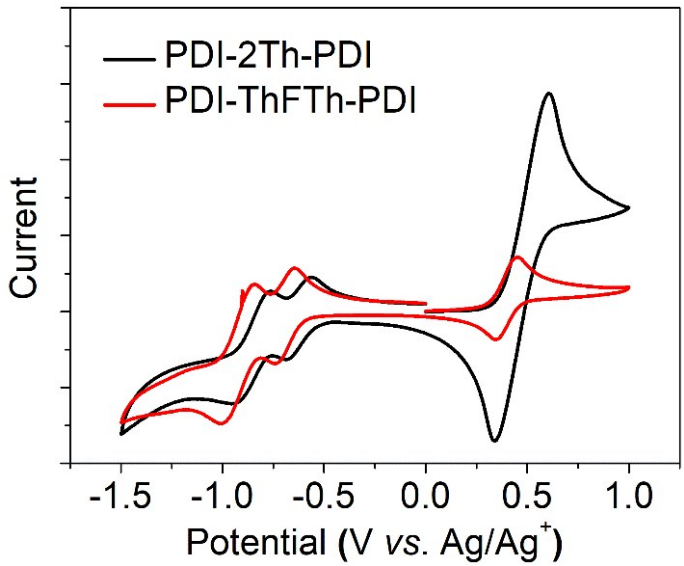

Fig. S3 Cyclic voltammograms of PDI-2Th-PDI and PDI-ThFTh-PDI film with Ag/Ag^+ as the reference.

Table S1 Summary of optical and electrochemical properties of PDI-2Th-PDI and PDI-ThFTh-PDI

Compound	λ_{max} (nm)	λ_{onset} (nm)	E_g^{opt} (eV)	E_{LUMO}^a (eV)	E_{HOMO}^b (eV)
PDI-2Th-PDI	229, 354, 458, 484, 525	640	1.94	-3.79	-5.73
PDI-ThFTh-PDI	230, 373, 459, 485, 527	651	1.90	-3.81	-5.71

[a] Obtained from CV data. [b] Obtained from the LUMO (CV data) and optical bandgap (E_g^{opt}).

5. Density functional theory (DFT) calculations

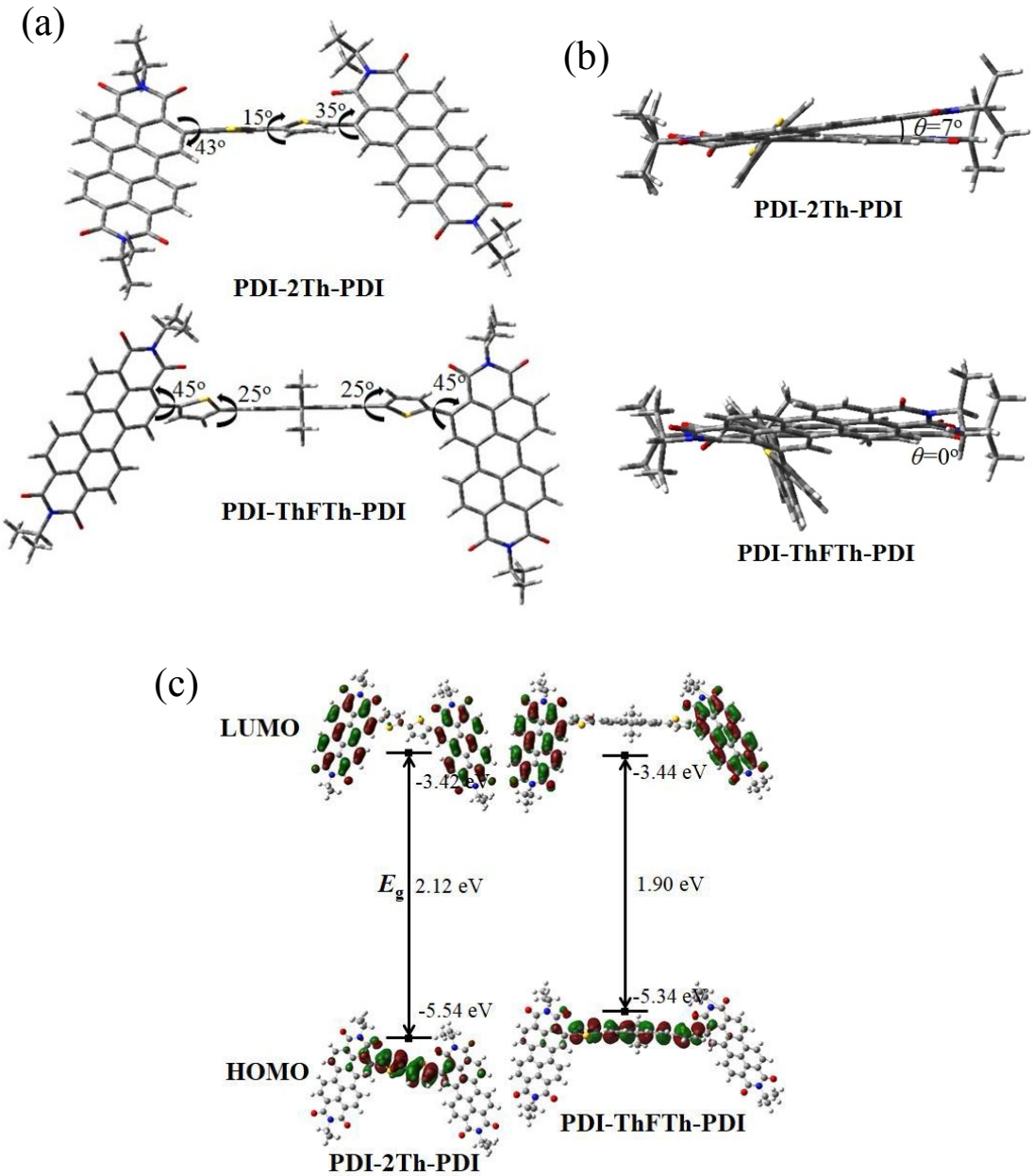

Fig. S4 Optimal molecular geometries from (a) front view and (b) side view of PDI-2Th-PDI and PDI-ThFTh-PDI. (c) Frontier molecular orbitals and HOMO-LUMO gaps of PDI-2Th-PDI and PDI-ThFTh-PDI.

As shown in Fig. S4a, for PDI-2Th-PDI, the dihedral angles between two PDIs on both sides with the neighboring thiophene rings were calculated to be about 43° and 35°. For PDI-ThFTh-PDI, the dihedral angle between PDI and thiophene plane is predicted to be 45°, while the dihedral angle between thiophene and fluorene plane are computed to be 25°. As shown in Fig. S4b, for the dihedral angles between the two constituent PDI units, we obtain 7° and 0° for PDI-2Th-PDI and PDI-ThFTh-PDI, respectively, which indicates that the structures of the two PDI molecules are almost planar.

We evaluated the structures using density functional theory (DFT) analysis utilizing Gaussian 09. DFT calculations are widely used to help understand the geometry and electronic properties of π-conjugated organic small molecules. For **PDI-2Th-PDI** and **PDI-ThFTh-PDI**, the frontier molecular orbitals and HOMO-LUMO gaps were optimized at the B3LYP/6-31G(d,p) level of theory, as shown in Fig. S4c.

6. Optimization of annealing conditions

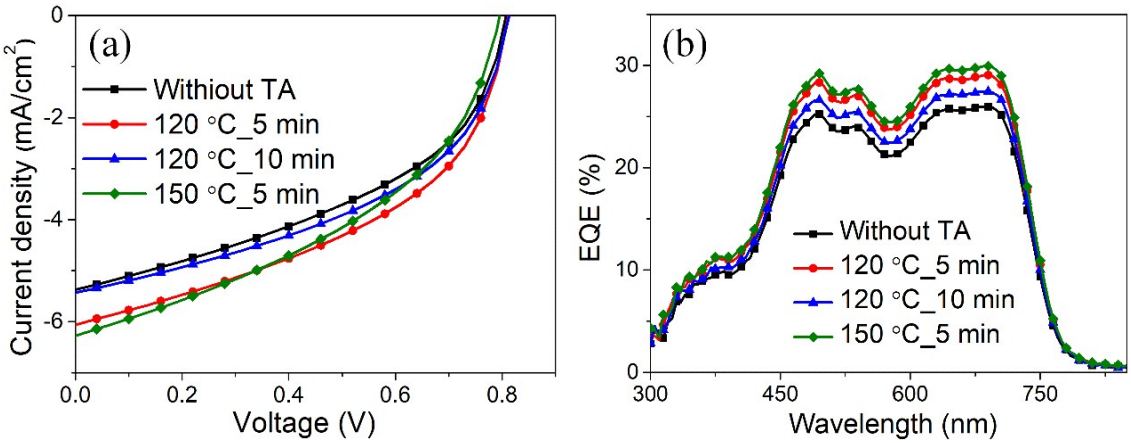

Fig. S5 (a) *J-V* characteristics, under 100 mW cm^{-2} illumination (AM 1.5 G), and (b) corresponding EQE curves of the PSCs based on PTB7-Th:PDI-2Th-PDI active layers with and without thermal annealing (TA) at different temperatures for different TA times.

Table S2 Photovoltaic performance of the PSCs based on PTB7-Th:PDI-2Th-PDI active layers (30 mg mL^{-1} and 2000 rpm) with and without TA at different temperatures for different TA times

Temperature (°C)	Time (min)	V_{oc}[a] (V)	J_{sc}[a] (mA cm^{-2})	FF[a] (%)	PCE[a] (%)	J_{sc}^{IPCE} (mA cm^{-2})
Without TA		0.80 (0.77 ± 0.03)	5.36 (5.33 ± 0.63)	44.3 (40.3 ± 2.7)	1.92 (1.56 ± 0.17)	5.31
120	5	0.81 (0.80 ± 0.01)	6.06 (5.85 ± 0.19)	45.9 (44.4 ± 1.8)	2.26 (2.09 ± 0.11)	5.95
	10	0.81 (0.80 ± 0.01)	5.42 (5.46 ± 0.16)	46.3 (43.0 ± 2.9)	2.04 (1.88 ± 0.18)	5.62
150	5	0.80 (0.79 ± 0.01)	6.27 (6.11 ± 0.43)	42.2 (40.0 ± 1.3)	2.11 (1.99 ± 0.13)	6.12

[a] The best values are given, followed by the averages and standard derivations in

parentheses, calculated from at least five devices.

7. Optimization of donor/acceptor (D/A) weight ratio

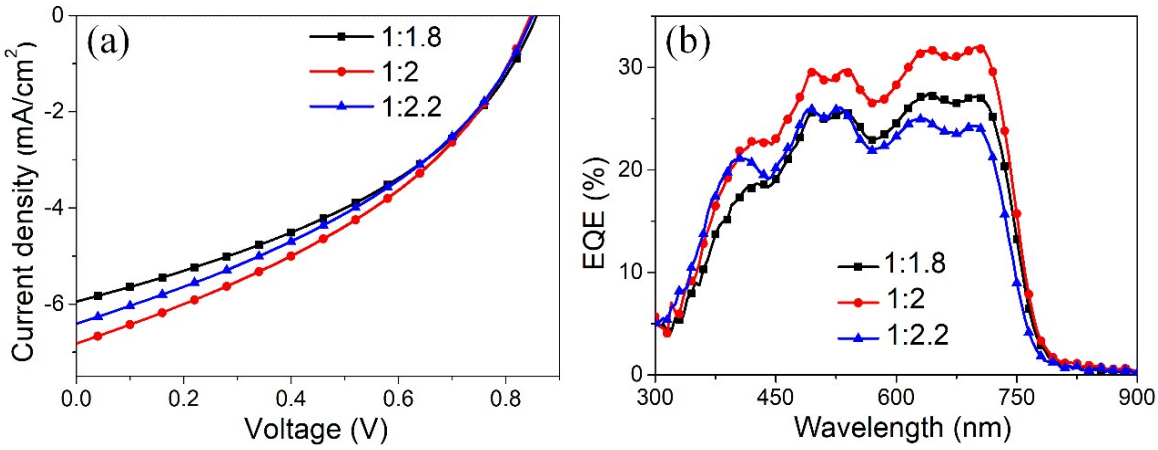

Fig. S6 (a) *J-V* characteristics, under 100 mW cm^{-2} illumination (AM 1.5 G), and (b) corresponding EQE curves of the PSCs based on PTB7-Th:PDI-ThFTh-PDI active layers with different donor/acceptor (D/A) weight ratios.

Table S3 Photovoltaic performance of the PSCs based on PTB7-Th:PDI-ThFTh-PDI active layers with different D/A weight ratios

Ratio (w/w)	V_{oc}[a] (V)	J_{sc}[a] (mA cm^{-2})	FF[a] (%)	PCE[a] (%)	J_{sc}^{IPCE} (mA cm^{-2})
1:1.8	0.86 (0.86 ± 0.01)	5.89 (5.84 ± 0.13)	40.3 (40.2 ± 0.4)	2.05 (2.01 ± 0.03)	5.80
1:2	0.84	6.81 (6.47 ± 0.24)	39.0 (39.3 ± 0.5)	2.22 (2.14 ± 0.06)	6.79
1:2.2	0.85 (0.86 ± 0.01)	6.41 (5.67 ± 0.11)	38.4 (41.3 ± 1.3)	2.10 (2.06 ± 0.02)	5.56

[a] The best values are given, followed by the averages and standard derivations in parentheses, calculated from at least five devices.

8. Optimization of solution concentration and spin-rate

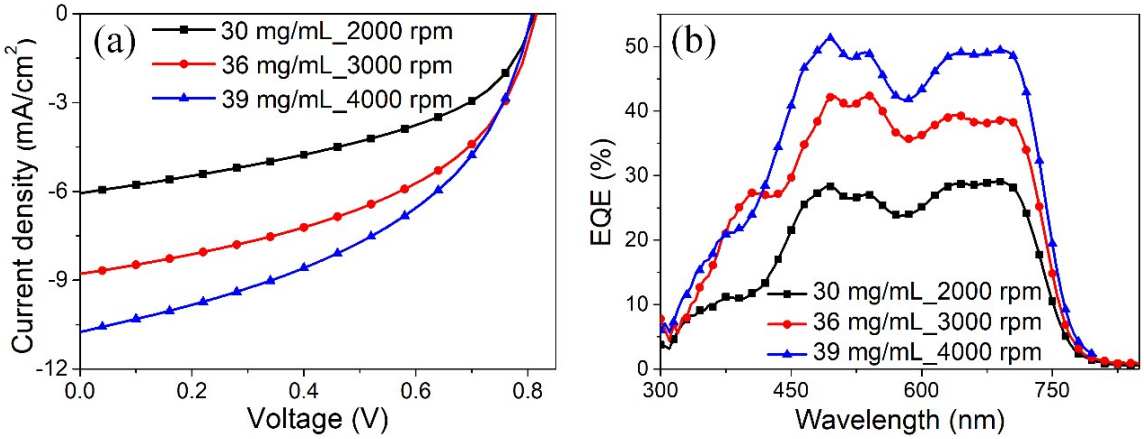

Fig. S7 (a) *J-V* characteristics, under the illumination of AM 1.5 G, 100 mW cm^{-2}, and (b) corresponding EQE curves of the PSCs based on PTB7-Th:PDI-2Th-PDI active layers processed at different solution concentrations and spin rates.

Table S4 Photovoltaic performance of the PSCs based on PTB7-Th:PDI-2Th-PDI active layers processed at different solution concentrations and spin rates

Concentration (mg mL^{-1})	Spin-rates (rpm)	V_{oc}[a] (V)	J_{sc}[a] (mA cm^{-2})	FF[a] (%)	PCE[a] (%)	J_{sc}^{IPCE} (mA cm^{-2})
30	2000	0.81 (0.80 ± 0.01)	6.06 (5.85 ± 0.19)	45.9 (44.4 ± 0.8)	2.26 (2.09 ± 0.11)	5.95
36	3000	0.83	8.75 (8.36 ± 0.31)	47.1 (46.5 ± 2.3)	3.44 (3.31 ± 0.12)	8.66
39	4000	0.81 (0.81 ± 0.01)	10.72 (10.08 ± 0.38)	46.0 (46.7 ± 0.6)	4.00 (3.82 ± 0.10)	10.50

[a] The best values are given, followed by the averages and standard derivations in parentheses, calculated from at least eight devices.

9. X-ray diffraction (XRD) patterns

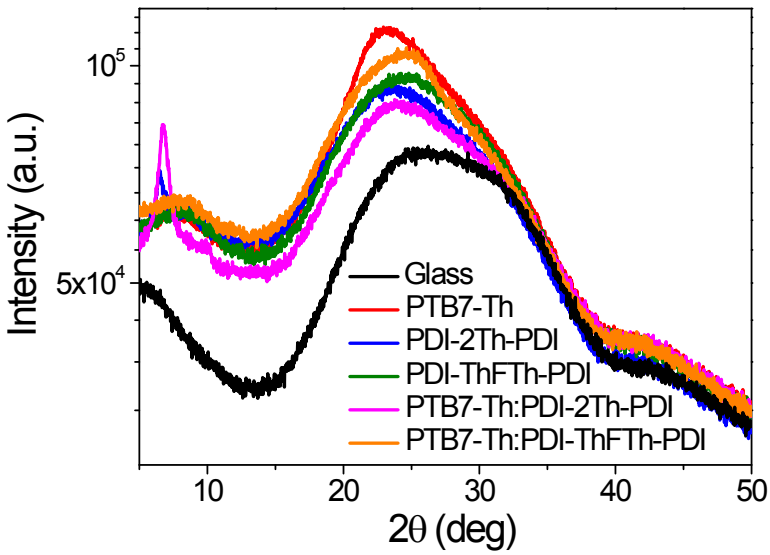

Fig. S8 X-ray diffraction (XRD) patterns of neat PTB7-Th, PDI-2Th-PDI, PDI-ThFTh-PDI, and PTB7-Th:PDI-2Th-PDI (or PDI-ThFTh-PDI) blend films on glass substrates annealed at 120 °C for 5 min. The XRD of glass is also measured for comparison.

10. ^{1}H and ^{13}C NMR spectra

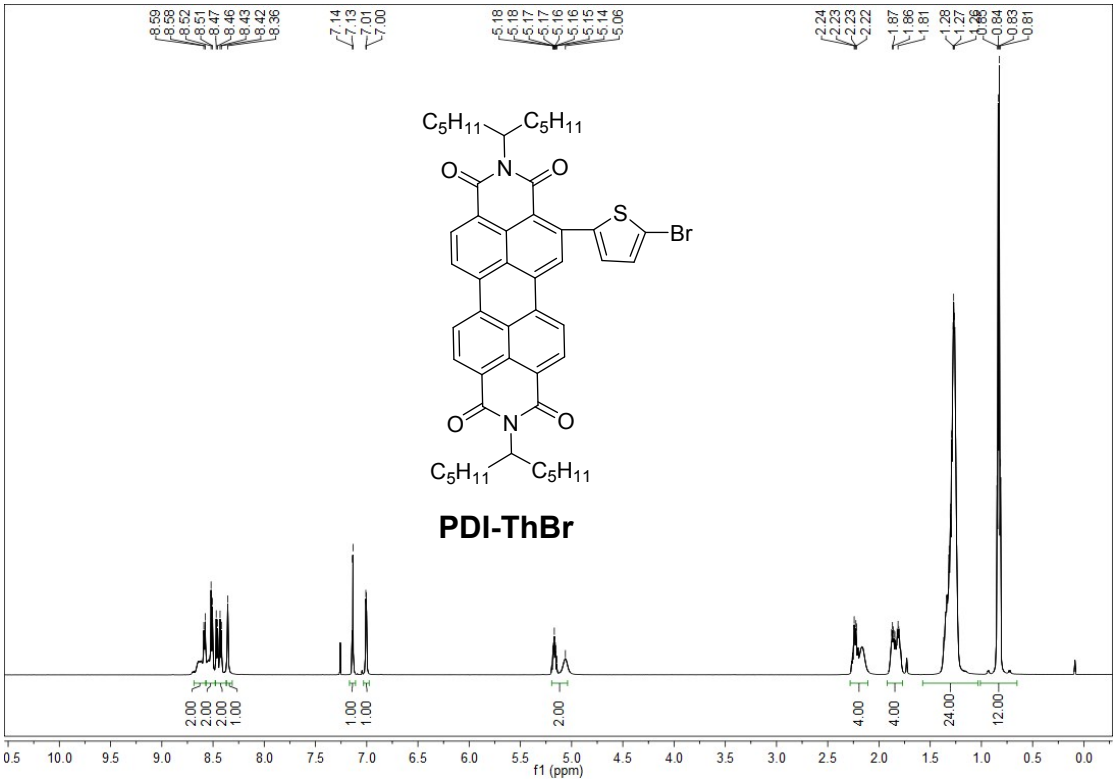

Fig. S9 ^{1}H NMR of **PDI-ThBr.**

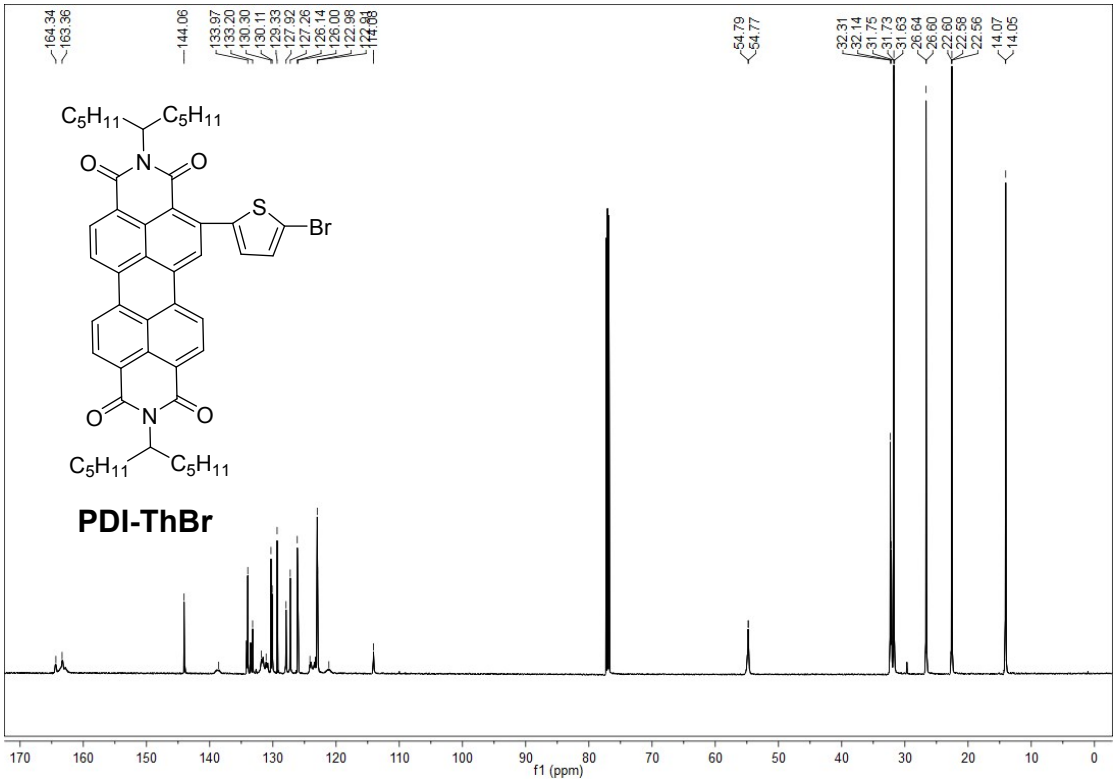

Fig. S10 ^{13}C NMR of **PDI-ThBr.**

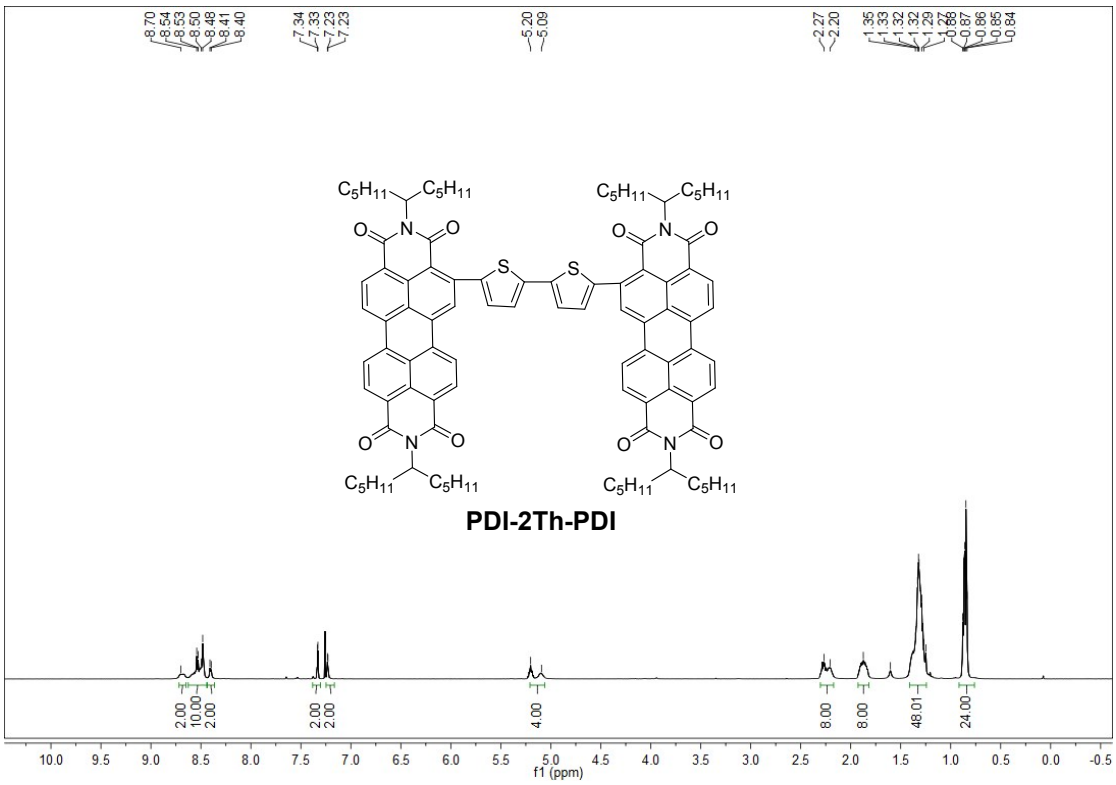

Fig. S11 ^{1}H NMR of **PDI-2Th-PDI.**

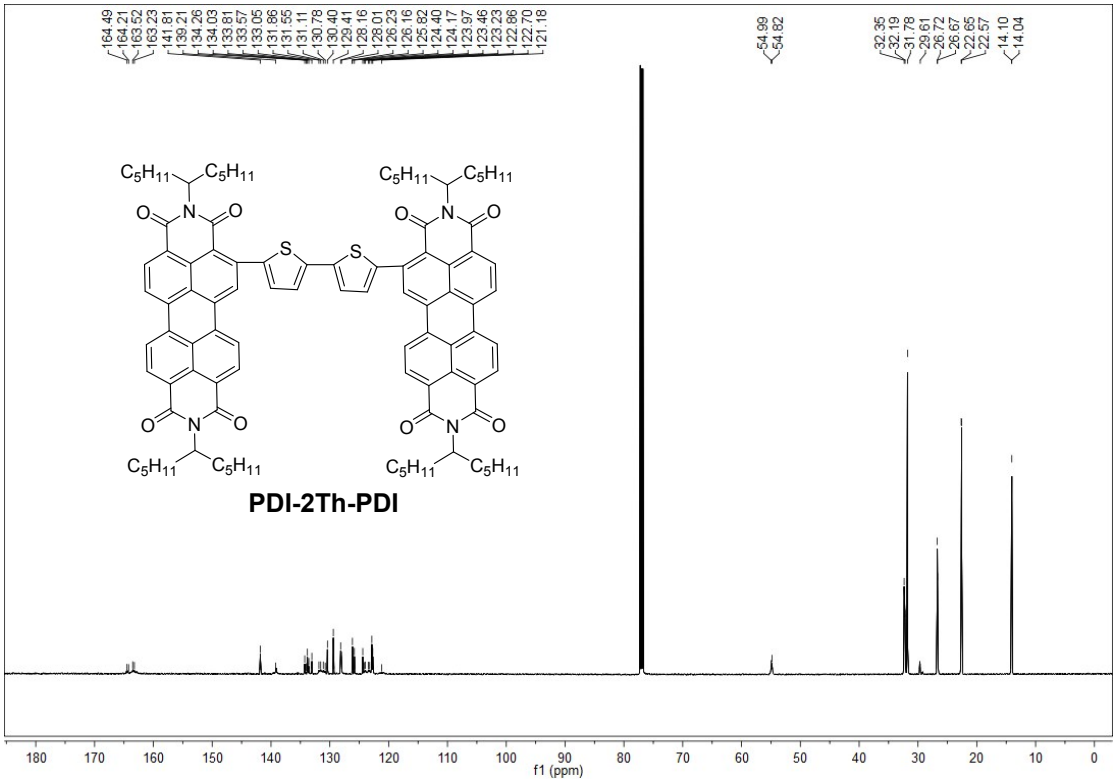

Fig. S12 ^{13}C NMR of **PDI-2Th-PDI.**

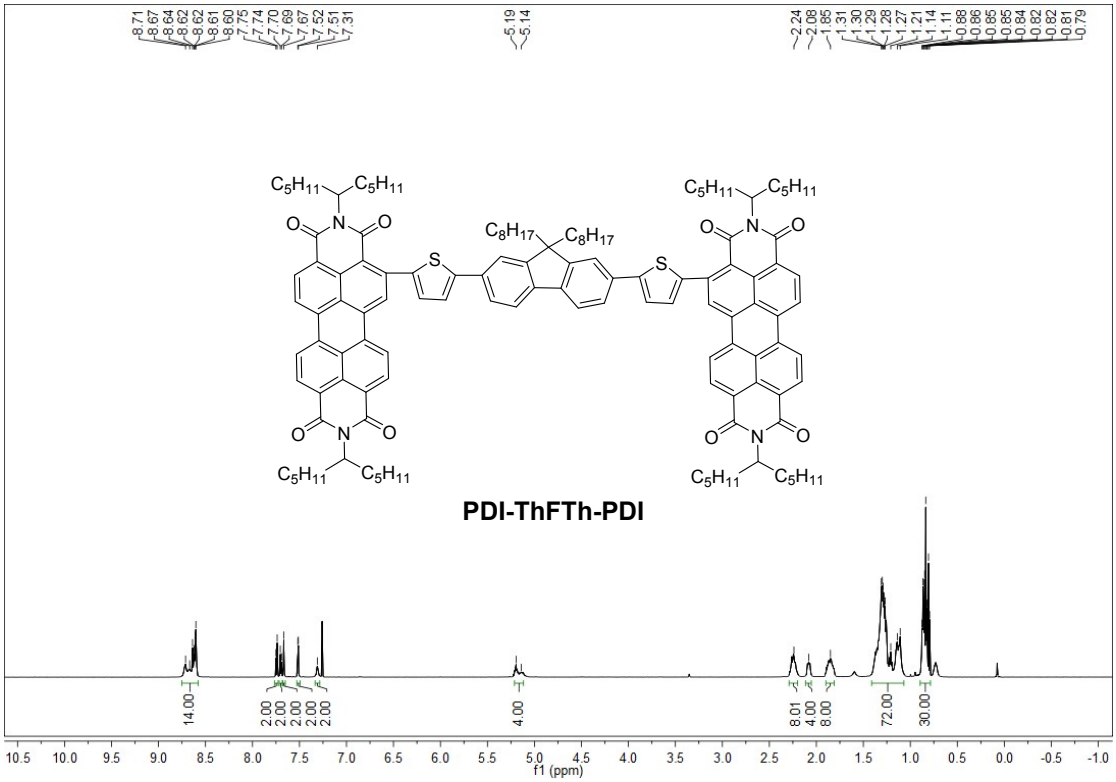

Fig. S13 ^{1}H NMR of **PDI-ThFTh-PDI.**

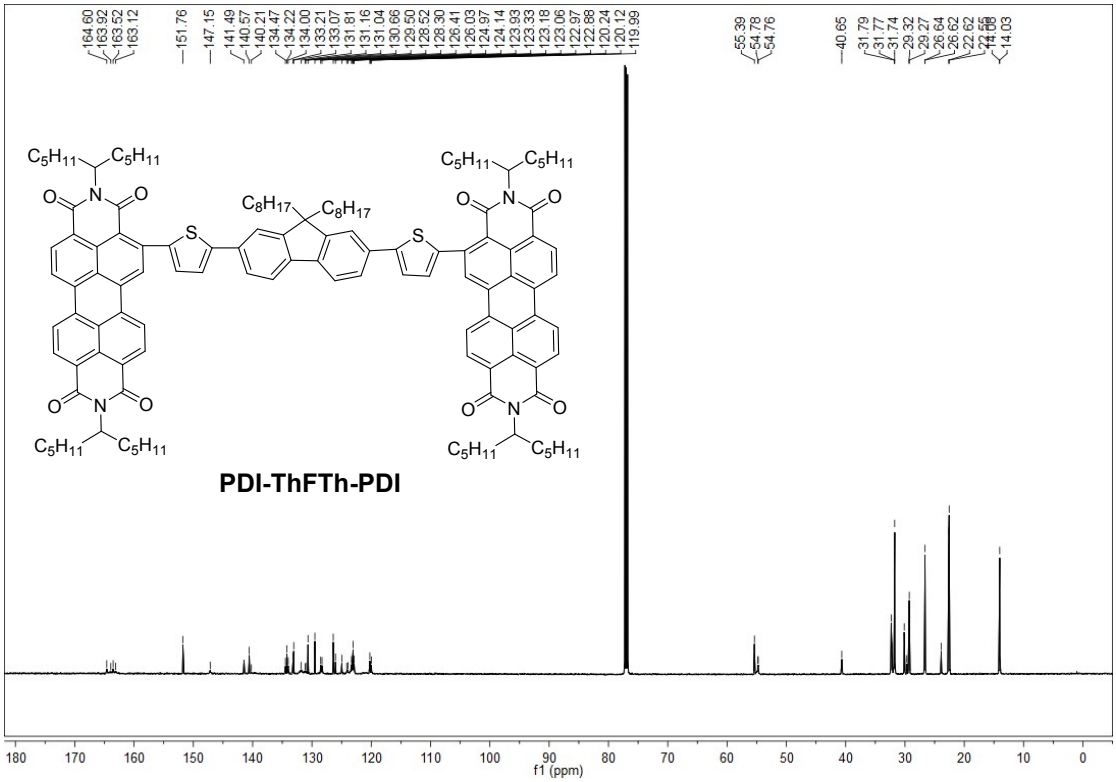

Fig. S14 ^{13}C NMR of **PDI-ThFTh-PDI.**